Improving the Prediction Accuracy of Groundwater Salinity Mapping Using Indicator Kriging Method

Abdelhamid Bradaï[1]; Abdelkader Douaoui[2]; Naïma Bettahar[3]; and Ibrahim Yahiaoui[4]

Abstract: The saline groundwater irrigation is an important problem in the arid and semiarid region because it can cause soil salinization and reduce crop productivity. The accurate spatial distribution of groundwater salinity can be helpful to managers and decision makers. In this study, the mapping of salinity risk through groundwater electrical conductivity (EC) irrigation was performed based on data collected from 88 wells in the Lower-Cheliff plain (Algeria). The EC data showed a normal distribution based on elementary statistics. The EC classified using Riverside method point out a high risk of groundwater salinity (Class C3) or very high risk (Class C4) for soil salinization. The EC estimated by ordinary kriging method (OK) revealed on one hand, an underprediction of a high value, on the other hand, an overprediction of low value. The methodology of nonparametric and nonlinear of indicator kriging (IK) was performed by three thresholds: EC > 2.25, EC > 3, and EC > 5 dS/m. The map has been obtained from the combination of the local conditional cumulative distribution function (CCDF). The interpolated map by IK indicates the same overall spatial distribution of salinity with the one obtained by OK, enlightening differences in the shape and size of the area. The comparison between the groundwater EC estimated by OK and the one using IK demonstrates that IK has a better spatial prediction of salinity in terms of area and uncertainty. The groundwater salinity map was improved and accurately predicted by IK interpolation method. **DOI: 10.1061/(ASCE)IR.1943-4774.0001019.** © *2016 American Society of Civil Engineers.*

Author keywords: Groundwater; Irrigation; Salinity; Map; Ordinary kriging; Indicator kriging.

Introduction

Water scarcity and groundwater salinity are major constrains for the agricultural production of the semiarid region of the Lower-Cheliff plain (northwestern Algeria). The groundwater supply is the primary water resource for irrigation in the area (Bouarfa et al. 2009; Bradaï et al. 2012). However, irrigation using saline groundwater can alter soil proprieties, causing salinization and reducing crop productivity (Ramsis et al. 1999). The use of groundwater resources has dramatically increased during the last decades (Amichi et al. 2012), leading to a continuous salinization process of the topsoil (Douaoui et al. 2006; Douaoui and Lepinard 2010). Therefore, an accurate mapping of groundwater salinity in an aquifer is very important to managing the irrigation in the area.

The control and the management of groundwater irrigation (aquifer salinity and pollution risk) is essential through the application of legitimate digital methods (Goovaerts et al. 2005; Assaf and Saadeh 2009; Mendes and Ribeiro 2010). In this study, the applied methods gave rise to results in the form of digital maps to facilitate their interpretation. These maps need to be adjusted with the right spatial analysis, to ensure an accurate digital mapping of groundwater quality.

The adopted digital mapping is based on kriging, which is a geostatistical interpolation technique that deals with many variations, including simple kriging (SK), ordinary kriging (OK), cokriging (CK), and nonlinear kriging (NK). Among those, ordinary kriging (OK) is frequently the most used (Douaoui et al. 2006; Hooshmand et al. 2011). Now, there are many examples of OK to estimate groundwater salinity variables at nonsampled sites from data of adjacent sample points (Theodossiou and Latinopoulos 2007; Yimit et al. 2011; Hooshmand et al. 2011). However, the linear prediction methods, i.e., OK, do not contribute truly as an effective solution, because the krigged values $Z^*(x_0)$ are affected by smoothing effect, as consequence of prediction errors (Deutsch and Journel 1998; Lloyd and Atkinson 2001; Chica-Olmo et al. 2014). Consequently, the expected results regarding the determination $Z^*(x_0) > Z_c$, by applying a limit value Z_c to the krigged values $Z^*(x_0)$, could be biased. This bias depends on the value of Z_c.

Facing this situation, the prediction of a local conditional cumulative distribution function (CCDF), of $Z^*(x_0) > Z_c/Z(x_i)$, $i = 1, \ldots, n$, is a better solution instead of estimating the most likely value at an unsampled location by linear kriging x_0 (Chica-Olmo et al. 2014). This function allows us to estimate the spatial probability when the value $Z^*(x_0)$ exceeds a threshold value Z_c at an unsampled location conditional to the experimental field information x_0, $Z(x_i)$, $i = 1, \ldots, n$. It is a nonlinear prediction problem. A geostatistical application is the solution through the use of nonparametric methods such as indicator kriging (IK) (Triantafilis et al. 2004; Adhikary et al. 2011; Antunes and Albuquerque 2013). In recent studies, IK is used to analyze the spatial variability of groundwater salinity; whereas Kuisi et al. (2009) used OK in addition to IK for the same purpose in the

[1]Institute of Agricultural Sciences and Laboratory of Water and Environment, Dept. of Hydraulics, Architecture and Civil Engineering Faculty, Univ. of Hassiba Ben Bouali, Chlef 02000, Algeria; Agricultural Sciences Institute, Hay Salam Box No. 151, Chlef 02000, Algeria (corresponding author). E-mail: bradai.hamid@gmail.com; a.bradai@univ-chlef.dz

[2]Univ. Center of Morsli Abdellah, Tipaza 42000, Algeria; Laboratory of Crop Production and Sustainable Valorization of Natural Resources, Univ. of Djilali Bounaama-Khemis Miliana, Ain-Defla 44225, Algeria.

[3]Dept. of Hydraulics, Architecture and Civil Engineering Faculty, Univ. of Hassiba Ben Bouali, Chlef 02000, Algeria; Laboratory of Water and Environment, Univ. of Hassiba Ben Bouali, Chlef 02000, Algeria.

[4]Laboratory of Crop Production and Sustainable Valorization of Natural Resources, Univ. of Djilali Bounaama-Khemis Miliana, Ain-Defla 44225, Algeria; Faculty of Nature, Life, and Earth Sciences, Univ. of Djilali Bounaama-Khemis Miliana, Ain-Defla 44225, Algeria.

Note. This manuscript was submitted on August 7, 2015; approved on December 17, 2015; published online on April 1, 2016. Discussion period open until September 1, 2016; separate discussions must be submitted for individual papers. This paper is part of the ***Journal of Irrigation and Drainage Engineering***, © ASCE, ISSN 0733-9437.

Amman-Zarqa Basin, and Dash et al. (2010) applied it for groundwater depth and quality parameters in Delhi. Also, Arslan (2012) used OK and IK to analyze the spatial and temporal groundwater salinity in Bafra plain (Turkey).

All those studies applied the IK method to estimate the likelihoods for the variables that exceeded a specified value (threshold) (Demir et al. 2008). This paper presents the application of the IK method in the spatial prediction of a categorical variable (Journel 1983, 1986; Solow 1993; Walter 1993; Goovaerts and Journel 1995), related to the groundwater salinity. The purpose of this paper on one hand, is to combine the estimated values of different salinity classes; obtaining a discrete version of the CCDF which represents the expected value of the rank of the electrical conductivity (EC) threshold at a sampled point, and then, to improve the prediction accuracy of groundwater salinity that is potentially used for irrigation in the Lower-Cheliff plain, both linear and nonlinear interpolation were used, the efficiency of both methods was assessed, and the best one was determined.

Materials and Methods

Study Area

The Lower-Cheliff plain is one of the regions most affected by soil salinity in Algeria. It extends over 60,000 ha of area, including 40,000 ha of irrigation schemes around the localities of Ouarizane, Djdiouia, Hmadna, and Guerouaou. It is located in the northwest of Algeria (0°40′ and 01°06′08″ E and latitudes 34°03′12″ and 36°05′57″ N) (Fig. 1). The specific semiarid climate of the Lower-Cheliff comes with very hot summers and cold winters, and also moderate rainfalls and evaporation intensities of 250 and 1,939 mm/year, respectively (Hartani et al. 2012). According to Douaoui et al. (2001), the soils are limey with clayey texture. Yahiaoui et al. (2015), have revealed the soils salinization can go back to the saliferous formation of Trias and Miocene, and the salinization phenomena has been accelerated in the last two decades following the increased utilization of groundwater irrigation. Crops patterns in the study area vary considerably: artichoke, melon, olive, pomegranate, and citrus trees cropped during irrigation period; barley and wheat are also cropped during the rainy season.

Historically, the small basin called Merdjet Sidi Abed and the Gargar dam were the only water supplies for irrigation in the area. Hence, the long dryness periods have significantly influenced these resources and an alternative was more needed than before. As the area lies on an important potential of groundwater resource (Bouarfa et al. 2009), wells canals were introduced by farmers and new volumes were available for cropping practices. As a result, groundwater irrigation became the main water supply in the Lower-Cheliff. However, Bradaï et al. (2012) have assessed that "these waters have normally high salinity and are unusable for irrigation" concluding that "they carry a great danger of salinization." The used irrigation system is mainly based on border-and-furrow methods.

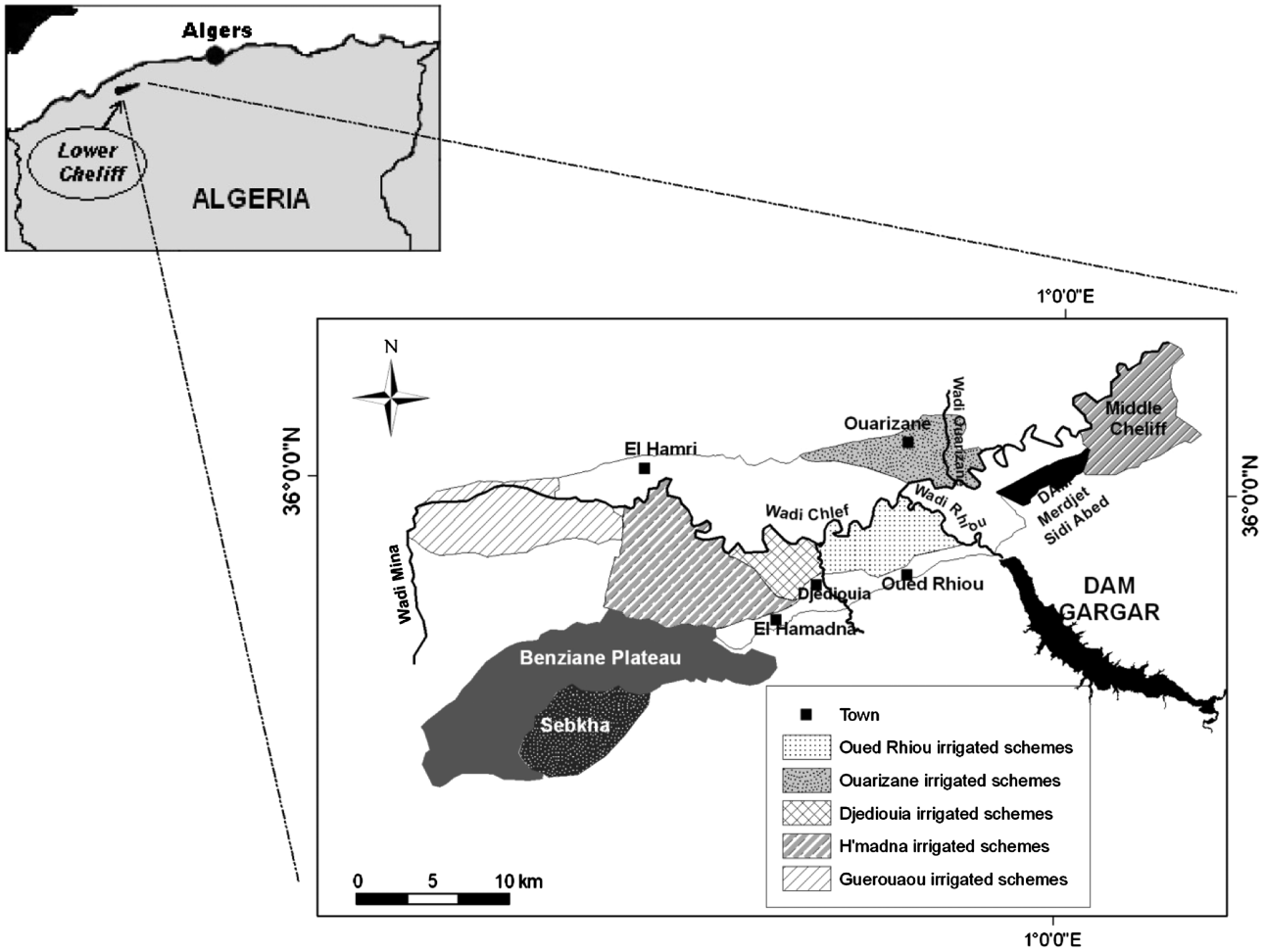

Fig. 1. Main irrigation scheme in the Lower-Cheliff plain

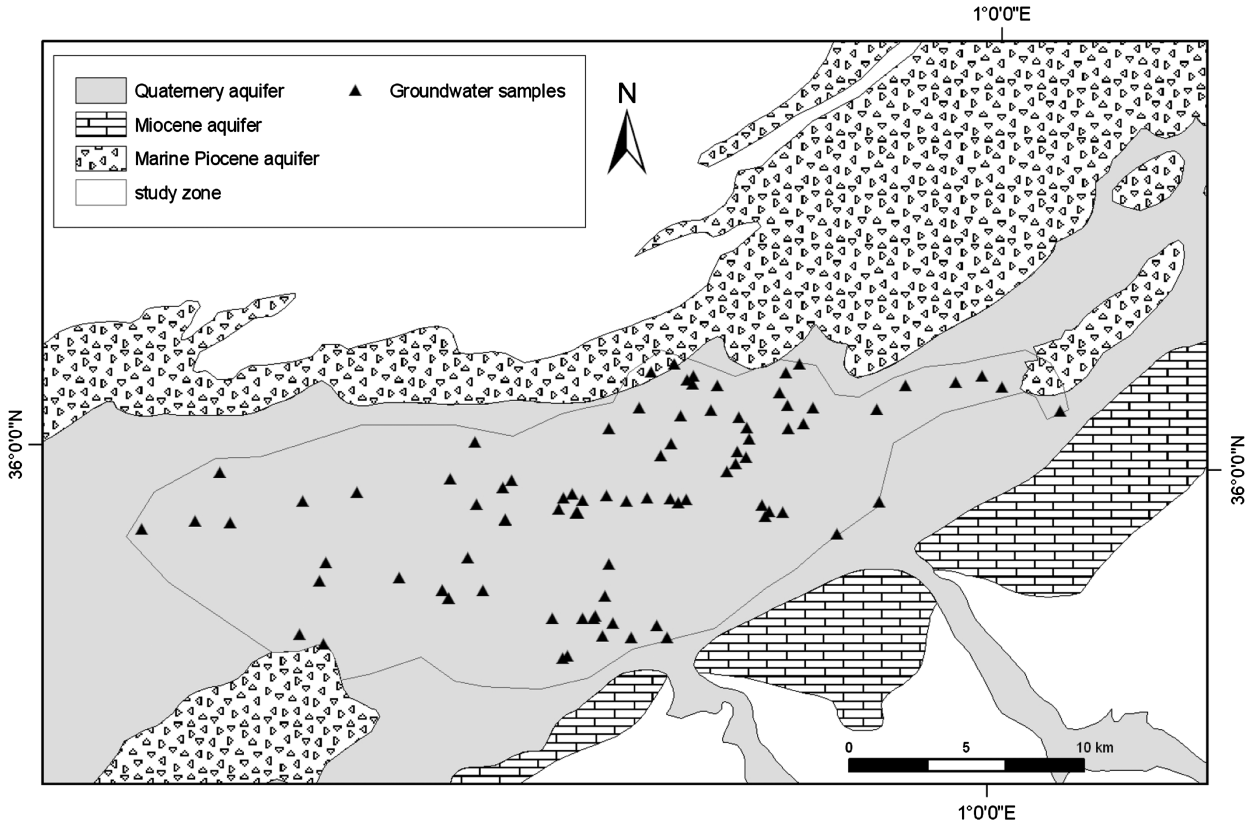

Fig. 2. Distribution of the collected samples and the main aquifers in the study area

Groundwater Samples Collection

The groundwater resources are originally coming from three main aquifers in the study area (Bradaï et al. 2012) (Fig. 2): (1) the Miocene aquifer, which extends along the southern boundary of the plain consisting of sandstone and limestone of Lithotamnium; (2) the Marine Pliocene aquifer which is a sequence of clays and marls with thin layers of sandstone exposed in the northern plain; and (3) the Quaternary Pliocene continental aquifer composed of sediments consisting of clay-based marl and beds of sand, gravel, and conglomerates. It is considered the most important aquifer and it is located in the center of the plain.

Groundwater samples were collected using a GPS device during May and June 2009 from 88 wells distributed along the area (Fig. 2). The wells' depths are between 60 and 120 m. All the sampling wells are usually used in irrigation by farmers and come from the Quaternary Pliocene continental aquifer. Then, the EC is measured in dS/m for all the collected samples using handy devices on the field [WTW 350i (Wissenschaftlich-Technische Werkstätten, Weilheim, Germany), ±0.5% of precision].

Table 1 provides a summary of groundwater salinity statistics. The groundwater EC varies between 1.2 and 7.03 dS/m, with a mean value of 3.34 dS/m. The variance is 2.34 and a standard deviation of 1.56 dS/m, explaining the spatial heterogeneity of the used data [Fig. 4(a)].

Assessment of the Groundwater Salinity Used for Irrigation

According to Richards (1954), the measured EC values gave rise to a classification of the water salinity used for irrigation: (C1) low salinity (0–0,250 dS/m), can be used in most crops and soil types with a low hazard of salinization; (C2) medium salinity (0,250–0,750 dS/m), can be used moderately for crops that are moderately salt tolerant; (C3) high salinity (0,750–2,250 dS/m), cannot be used in areas with drainage deficiency, pushing to select crops that are considerably tolerant to salts even under good drainage conditions; (C4) very high salinity (2,250–5 dS/m), not appropriate for irrigation of common crops but can be used for a previous selection of crops in highly permeable, well-drained soils; and (C5) unusable water for irrigation (EC > 5 dS/m). In addition, Ayers and Wescot (1988), had recommended a 3 dS/m threshold after many experiments on crops, as an acceptable maximum for the majority of the crops.

Table 1. Statistical Analysis of the Groundwater Salinity

Statistical parameters	EC (dS/m)
Number of samples	88
Mean	3.34
Minimum	1.2
Maximum	7.03
SD	1.56
Variance	2.43
Coefficient of variation (%)	46.59
Skewness	0.55
Kurtosis	−0.7
Kolmogorov-Smirnov statistic	0.152
Kolmogorov-Smirnov significance	0

Geostatistical Analysis

Geostatistics involves the study of spatially correlated data used in geosciences. Spatial correlation is present in all natural phenomena. In earth sciences, samples taken at close distances to one another

tend to be more similar compared to samples taken from far located points. The geostatistical kriging technique allows the spatial correlations between samples to determine an average value at an unsampled location (Kasmaee et al. 2010). Geostatistical analysis consists of variography and kriging.

Variography

The main tool in geostatistics is the variogram, it expresses the spatial dependence between neighboring observations (Webster and Oliver 2001). The variogram (γ_h) can be defined as the semivariance of the difference between the attribute values for all separated points by h distance as follows:

$$\gamma_h = \frac{1}{2N(h)} \sum_{i=1}^{N(h)} [Z(x_i) - Z(x_i + h)]^2 \quad (1)$$

where (γ_h) = estimated or experimental semivariance value for all pairs at a lag distance h; $Z(x_i)$ = groundwater EC value per point i; $Z(x_i + h)$ = groundwater EC value (dS/m) for other separated points from x_i by a discrete distance h; x_i = georeferenced positions where the $Z(x_i)$ values were measured; and $N(h)$ represents the number of observation pairs for separated points by the distance h (Delhomme 1978).

The fitting of a theoretical semivariogram (curve) is an important step in the analysis. Hereby, the *sill* is the total variance σ^2 of the variable, the *range* is the maximal spatial extent of the spatial correlation between the observed variables, and the *nugget* is the random error. It can be also composed of nested models or structures, which commonly include nugget, spherical, exponential, Gaussian, and power models (Verfaillie et al. 2006).

The *VARIOWIN* software v2.2 (Pannatier 1996) was used to make the variogram and indicate the goodness of fit (IGF). The IGF is the number of standardization without units; it indicates a good fit when it is close to zero (Pannatier 1996).

Kriging

Kriging is a form of weighted average estimator. The weights are assigned on the basis of a model that fits a function, as the semivariogram represents the spatial structure in the searched variable (Lloyd and Atkinson 2001). However, kriging was proven as a powerful interpolation technique, it is recognized in many study fields and related disciplines such as: hydrogeology, hydrology, soil sciences, and mining sciences. (Akin and Siemes 1988). Various methods for kriging exist in geostatistics, among those the researchers applied both OK and IK.

Ordinary Kriging

The algorithm for OK uses a weighted linear combination of sampled points commonly situated inside a neighborhood around the location x_0

$$Z^*(x_0) = \sum_{i=1}^{n} \lambda_i Z(x_i) \quad (2)$$

and

$$\sum_{i=1}^{n} \lambda_i = 1 \quad (3)$$

where $Z^*(x_0)$ = estimated value by a location x_0; $Z(x_i)$ = available sample per location x_i, and λ_i is the weight assigned to the sample value; and n = number of considered samples in the prediction. To solve the equations induced by the search λ_i weight system, it is necessary to introduce the optimizing conditions (Delhomme 1978; Kumar 2007) of unbiasedness

$$E[Z^*(x_0) - Z(x_0)] = 0 \quad (4)$$

and minimum variance

$$\mathrm{Var}[Z^*(x_0) - Z(x_0)] = 0 \quad (5)$$

Indicator Kriging

The indicator kriging, initiated by Journel (1983), was then developed mathematically (Davis 1984; Cressie 1991; Bierkens and Burrough 1993). The basis of IK is to perform a spatial analysis, not directly from the targeted property, but through different functions from a binary coding as an indication to this property. The spatial variable interpolation method in IK, $Z(x_i)$, is transformed into an indicator variable with a binary distribution as follows:

$$I(x_i; Z_c) = \begin{cases} 1 & \text{if } Z(x_i) \geq Z_c \\ 0 & \text{if } Z(x_i) < Z_c \end{cases} \qquad i = 1, \ldots, n \quad (6)$$

where $I(x_i; Z_c)$ = indicator value at a location x_i; $Z(x_i)$ = measured value at a location x_i; and Z_c = threshold. The expected value of $I(x_i; Z_c)$, conditional on n surrounding data, can be expressed as

$$E[I(x_i; Z_c)] = \mathrm{Prob}[Z(x) \leq Z_c] = F(x_i; Z_c) \quad (7)$$

where $F(x_i; Z_c)$ = conditional cumulative distribution function (CCDF).

The function F represents the probability for an unknown value not exceeding a threshold Z_c. The CCDFs are modeled using a nonparametric (IK) approach (Eldeiry and Garcia 2011).

The interpolation can be performed using IK method in four steps:

1. The transformation of measured values in binary code (0-1) according to selected threshold value (Z_c) as in Eq. (5).
2. The calculation of the variogram for the conditional cumulative distribution function at a given threshold determines the spatial structure

$$\gamma^*(h; Z_c) = \frac{1}{2N(h)} \sum_{i=1}^{n} [(x_i; Z_c) - (x_i + h; Z_c)]^2 \quad (8)$$

3. After adjustment of the CCDFs variogram to a theoretical model, by applying the linear kriging in to a point (x_0) for $I(x_i, Z_c)$ using the equation

$$I*(x_0; Z_c) = \sum_{i=1}^{n} \lambda_i (x_i; Z_c) \quad (9)$$

where n = number of the experimental points considered in the prediction; and i = weight attributed to the experimental points.

This applied formula gives values from 0 to 1 through prediction at a given point of the probability, where the Z_i value is equal or less than the chosen threshold Z_c. The combination of these predictions, leads to the ability of having at each point, the probability where the variable is equal to the determined threshold value.

4. The last step consists of the prediction of the value $Z(x_0)$ for the Z property at a random point x_0, considering, its density function. This can be done through the calculation of the mathematical expectation of the property value following the procedure:

a. The difference between the predictions of CCDF for two followed threshold values allows determining the probability for each point. The realization of a discrete random variable named X, like the thresholds have been calculated at higher values, the calculation can be

$$\text{Probability}(x = Z_c) = \text{Probability}(x \geq Z_c) - \text{Probability}(x \geq Z_{c+1}) \quad (10)$$

where Z_c and Z_{c+1} are the two followed threshold values.

b. The combination of the thresholds values correspondent to different classes, obtains a discrete version of the repartition function that represents the mathematical expectation at the threshold level for the variable of a sampled point. The mathematical expectation is calculated using the formula

$$E(Z) = Z_c + 2Z_{c+1} + 3Z_{c+2} + 4Z_{c+3} + 5Z_{c+4} \quad (11)$$

Validation

This modeling was performed using 13 samples randomly extracted from the 88 total (15% from the sampling rate) (Fig. 3) to provide an accurate prediction. The standardized mean error (ME) should be close to 0 and the root-mean square error (RMSE) should be close to 1 (Arslan 2012). Mean error and root-mean square error were estimated using the following formulas:

$$ME = \frac{1}{nv}\sum_{i=1}^{nv} Z^*(x_i) - Z(x_i) \quad (12)$$

$$\text{RMSE} = \sqrt{\frac{[Z^*(x_i) - Z(x_i)}{nv}} \quad (13)$$

where $Z^*(x_i)$ = predicted value; $Z(x_i)$ = measured value; and nv = number of validation points.

Results and Discussion

Data Distribution

The kriging method works better on data with a normal distribution (Arslan 2012). No prior assumption is needed for IK about the distribution function for the studied variables (Walter 1993). The authors checked the distribution normality of the EC data using the Kolmogorov-Smirnov test. The asymmetry and the kurtosis values were close to zero with 0.55 and −0.70 respectively, which validate the normal distribution of the used data [Fig. 4(b)]. The statistic value of Kolmogorov-Smirnov test was highly significant with 0.152 (Table 1).

The frequency distribution of the groundwater EC (Table 2) shows that the Class C4 (very high risk) is dominant with 42 samples (47.7%). The Class C3 (high risk) represents 34.1% of samples. The Class C5, unusable water in irrigation, represents 18.2%. The Classes C1 and C2 (low and medium risk) are nonexistent in groundwater irrigation of Lower-Cheliff. However, more than half of the analyzed wells (51.1%) have a higher EC > 3 dS/m which is the maximum allowed level for most crops (Ayers and Wescot 1988). The use of groundwater that is potentially saline for irrigation in the study area can seriously damage the soil and the crops' yield.

Ordinary Kriging

The experimental omnidirectional variogram of the groundwater irrigation EC [Fig. 5(a)] indicates that the spherical variogram model better suited the groundwater EC. The nugget effect (C_0) was 1.199 $(\text{dS/m})^2$, the sill ($C_0 + C$) was 2.74$(\text{dS/m})^2$, and the range was 3,870 m. The spatial dependence of groundwater salinity can be classified according to nugget-to-sill ratio (%), with a ratio of <25% referring to a strong spatial dependence, a ratio of 25–75% indicating a moderate spatial dependence, and a ratio of >75% for a weak spatial dependence (Cambardella et al. 1994). The value for nugget-to-sill ratios was 49.3% in the present study, indicating the groundwater salinity has a moderate spatial dependence. The high value of the range indicates a spatial continuity of groundwater EC.

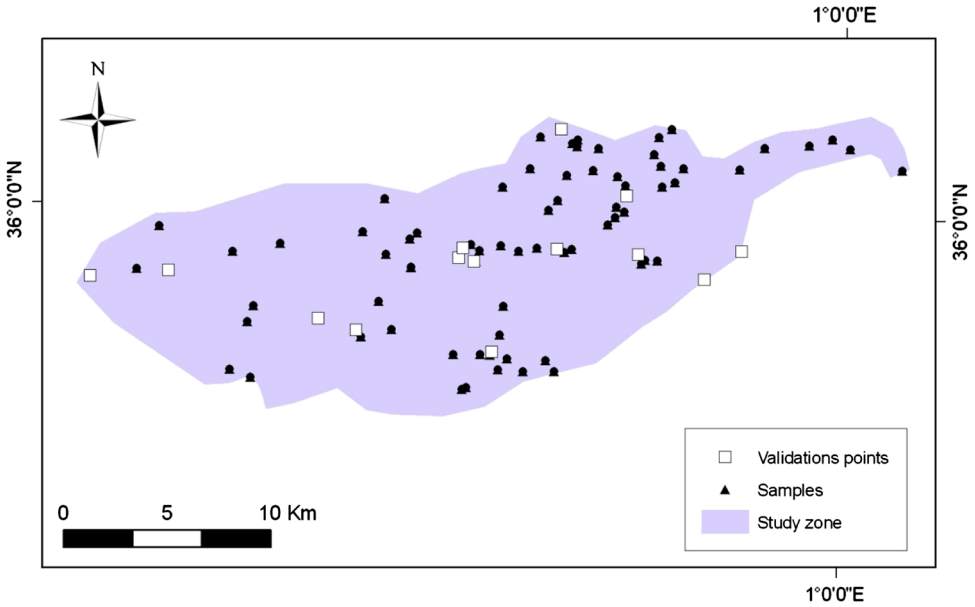

Fig. 3. Distribution of the selected points for validation

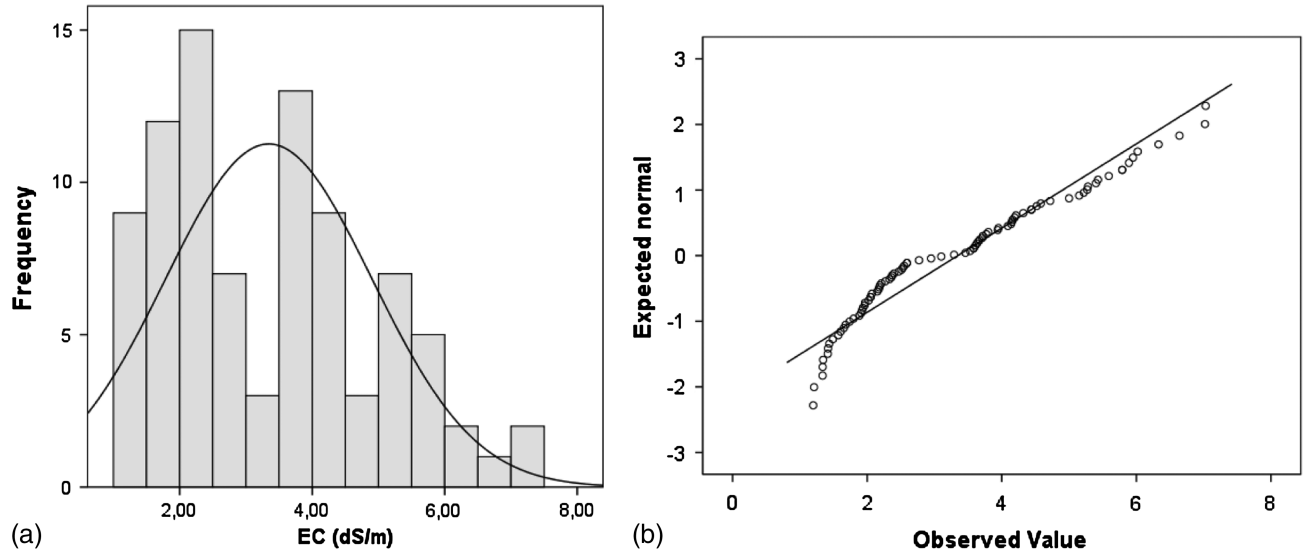

Fig. 4. (a) Frequency plot of the groundwater EC values; (b) scatter plot of the groundwater EC normal distribution

Table 2. Frequency Classification of the Groundwater Salinity

Class	C1	C2	C3	C4	C5	EC > 3 dS/m
N	0	0	30	42	16	45
Percentage	0	0	34.1	47.7	18.2	51.1

The groundwater irrigation has a high salinity risk. On one hand, the water with salinity between 3 and 5 dS/m is dominant in particular in the south- and north-east of the study area. On the other hand, the northwestern of the study area has a lower EC than 3 dS/m. The least salted water (EC < 2.25 dS/m) is localized in the center near the Cheliff Stream [Fig. 5(b)]. The water with very high risk (EC > 5 dS/m) is located at the southwestern and a little to the north of the area.

Indicator Kriging

Three thresholds were selected: 2.25, 3, and 5 dS/m. The first one is the higher limit of the Class 3 of USDA classification, in which exists the best class from the analyzed groundwater irrigation. The second threshold is the acceptable maximum threshold for the majority of the irrigated plants. The last one defines the threshold for unusable water in irrigation. From these three thresholds, four EC classes were retained: EC < 2.25, 2.25 < EC < 3, 3 < EC < 5, and EC > 5 dS/m.

These two models (Table 3) were selected as the best fits for different thresholds. The EC > 3 dS/m and EC > 5 dS/m were adjusted to fit the exponential model and EC > 2.25 was adjusted to fit the spherical model. The EC > 3 dS/m function had the biggest range with 4,940 m and the biggest nugget effect $0.066(\mathrm{dS/m})^2$. Moreover, the EC > 2.25 dS/m from the CCDF had the smaller range (2,469 m) and nugget effect $[0.045(\mathrm{dS/m})^2]$. The value for nugget-to-sill ratios for the three variograms indicates that EC > 2.25 and EC > 3 dS/m thresholds have a strong spatial dependence whereas the EC > 5 dS/m had a moderate one.

The results of the three EC thresholds enlighten us about the probability maps in Fig. 6. The study area has four classes of probability for the groundwater EC thresholds values. The comparison of the three maps is mainly based on the obtained surface area for each probability class (Table 4). The probability is accepted of 50% as a significance level, almost 80% of the studied area exceeds the threshold of 2.25 dS/m, giving a 61% of area with a very high probability (P > 75%). The 50/50 risk of exceeding a groundwater EC of 3 dS/m is 43% in the study area. It is localized to the south of the area where almost 20% exceeds the 5 dS/m threshold.

The theoretical variogram was calculated using the value of the mathematical expectation for the groundwater EC [Eq. (10)]. The variogram was adjusted to fit the exponential model [Fig. 7(a)], the nugget effect was $0.091(\mathrm{dS/m})^2$, the sill was $0.782\ (\mathrm{dS/m})^2$, and the range was 4,000 m with high spatial continuity. The nugget-to-sill ratio was 12.5% signifying strong spatial dependence of the value.

The obtained map of EC using IK [Fig. 7(b)] shows the same overall spatial distribution of salinity with the one obtained with OK, only this time the differences are mostly in the shape and size of the area.

Comparison between Ordinary and Indicator Kriging

Kriging is an optimal spatial regression technique that requires a spatial statistical model, popularly known as a semivariogram, representing the internal spatial structure of the data. It is known as the best linear unbiased estimator (BLUE). Ordinary kriging, one of the most common geospatial interpolation methods, is compared to IK in this study.

The performance of variography according to nugget-to-sill ratio (%) shows that the CCDFs were better than the indicator classes in presenting a good spatial structuring. Then, the nugget-to-sill ratio (%) of the mathematical expectation is very low compared to the variogram of OK. This result explains the good spatial correlation of the mathematical expectation for the groundwater.

The scatter plot of the measured groundwater EC and the estimated residue values (Fig. 8) using OK reveals an underestimation of the higher EC value and an overprediction of the lower value of groundwater EC. This underestimation is for an EC value equal to 3 dS/m. According to Douaoui et al. (2006), there is a sort of prediction problem using OK, in particular with the high values which are often underestimated.

The class of EC < 2.25 dS/m (low values) dropped from 5.81% with OK to 1.55% with IK (Table 5). This class was overestimated by OK. The second one, 2.25 < EC < 3 dS/m, increased with almost 4% for IK; going from 34.55% with OK to 38.05% using IK.

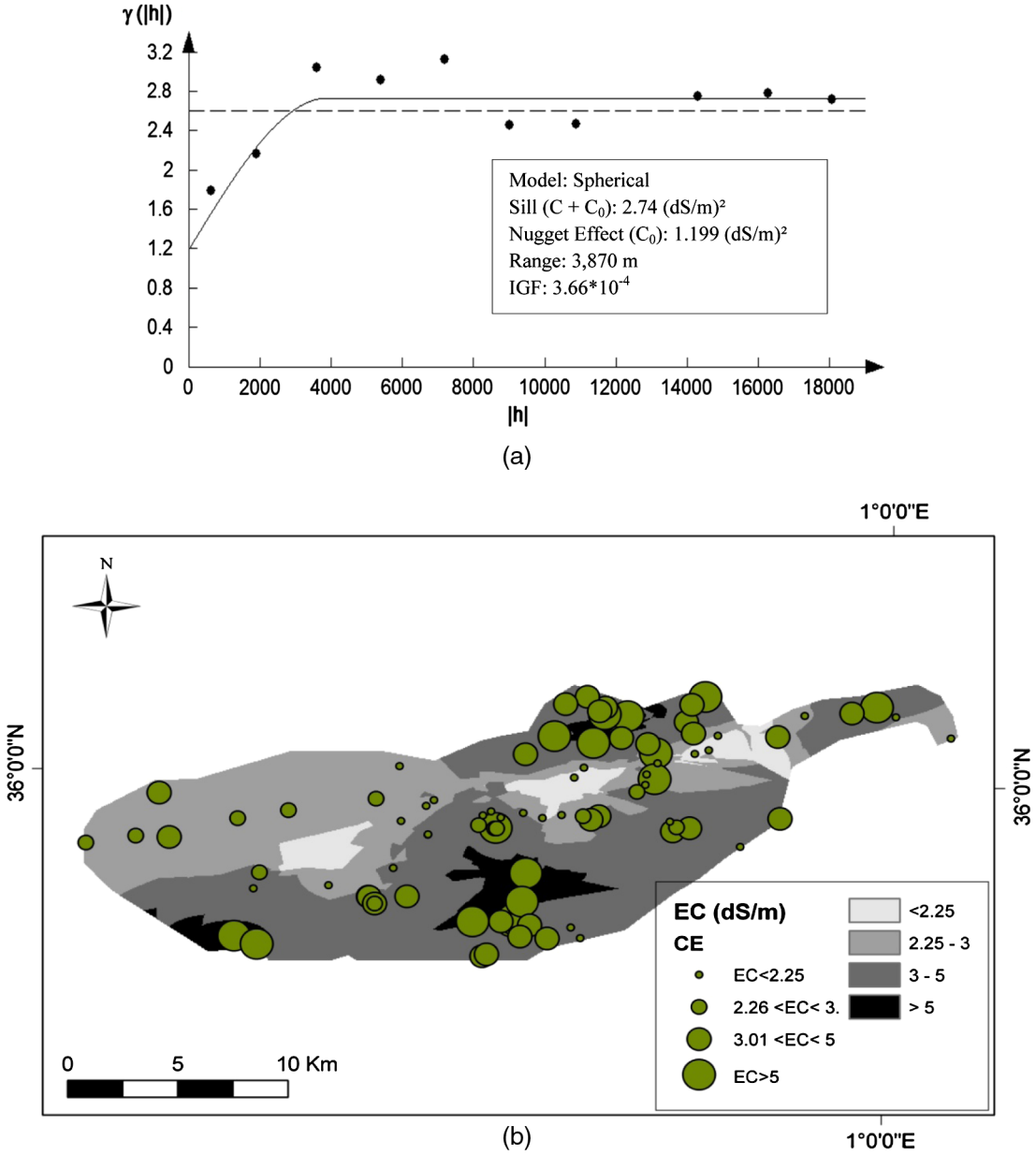

Fig. 5. (a) Omnidirectional variogram of the predicted EC; (b) prediction map of groundwater EC using OK

Table 3. Parameters of the Variogram Models of EC Thresholds (IK)

Thresholds	Model	Range (m)	Sill $(C_0 + C)$ $(dS/m)^2$	Nugget effect $(dS/m)^2$	Nugget ratio (%)	IGF
EC > 2.25	Spherical	2,469	0.223	0.045	20.18	1.96×10^{-4}
EC > 3	Exponential	4,940	0.264	0.066	24.99	1.78×10^{-3}
EC > 5	Exponential	3,060	0.181	0.054	29.83	3.60×10^{-3}

This confirms the underestimation of the class estimated using OK method. The high class of EC (EC > 5 dS/m) increased almost twice using IK method (Table 5). The estimated surface area using OK was 7.26% and the one with IK was 12.89%. This class was underestimated by OK.

The spatial distribution of groundwater EC classes obtained using IK defines areas where the EC is very high, which are also similar to those obtained by OK but with more details. An important range representing the high EC classes using IK (EC > 5 dS/m) (Table 5) is clearly observed in the north and south of the study area unlike the classes from OK. Meanwhile, the OK prediction revealed remarkable underprediction for the high values classes presenting a big hazard. The high surface retained using IK for the EC values under 5 dS/m, leads to compare this result to the OK one, the authors found that the underpredictions for this type of kriging (IK) are less important, giving a good precision quality that IK offers in the prediction of groundwater salinity hazard.

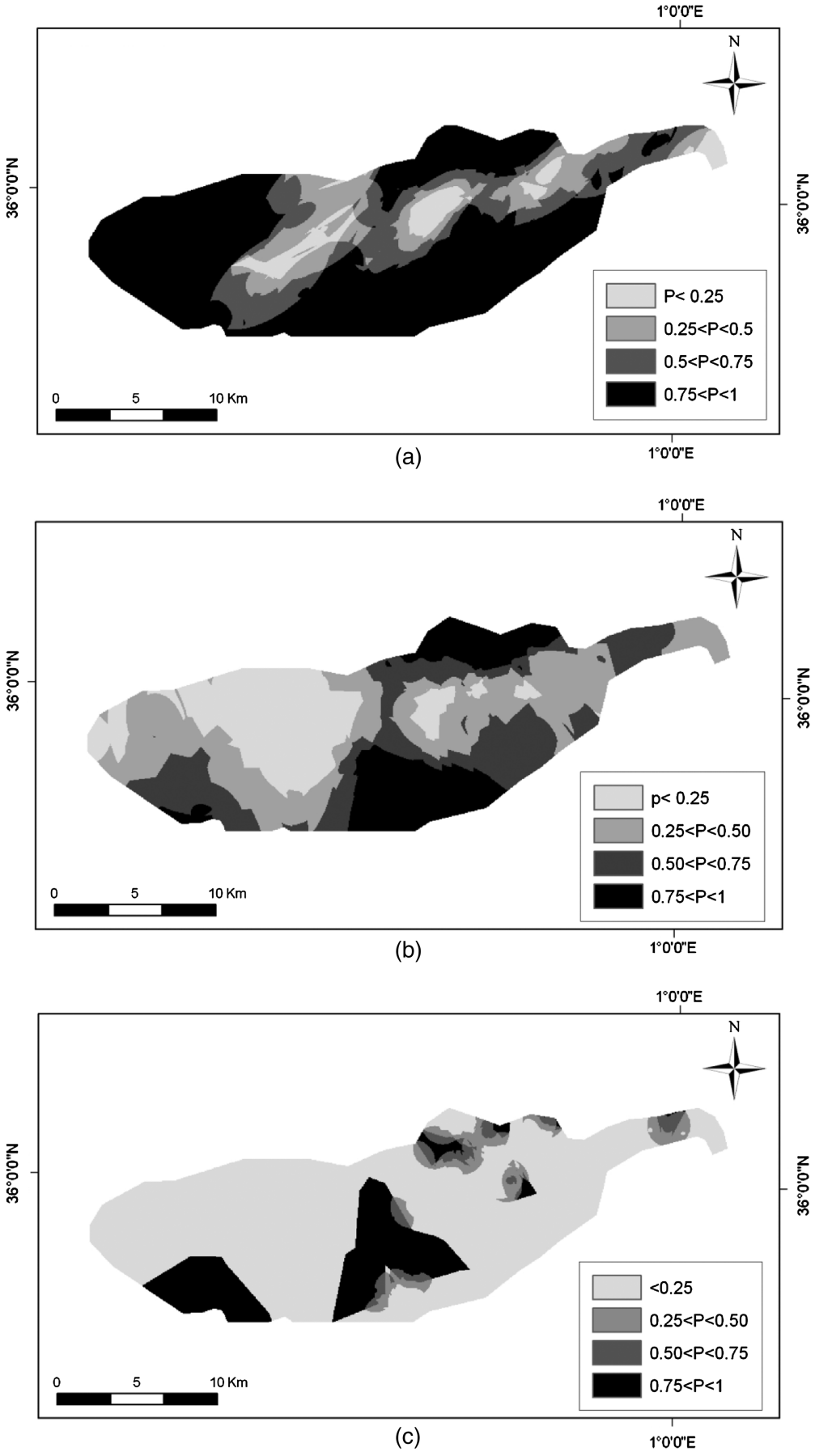

Fig. 6. Probability map of groundwater salinity spatial distribution with (a) EC > 2.25 dS/m; (b) EC > 3 dS/m; (c) EC > 5 dS/m

Table 4. Ranges of Probabilities of the Areas Exceeding the EC Thresholds

Probabilities (%)	Area (%)		
	EC > 2.25 dS/m	EC > 3 dS/m	EC > 5 dS/m
$P < 25$	6.4	23.3	74.6
$25 < P < 50$	14	33.9	5.1
$50 < P < 75$	18.6	25	3.3
$75 < P < 100$	61	17.8	17

The comparison of the two estimated maps by OK and IK shows that they have the same general structure, but the IK map shows a better smooth reappearance. Thus, for a sample initially identical, both methods lead to different prediction maps.

The cross-validation statistic shows how groundwater EC can be significantly estimated using the IK method more than using OK. Indeed, the mean error (ME) and the root-mean square error (RMSE) calculated for the two types of kriging give advantage to the IK (Table 6).

The final maps show that 60% of the aquifer's surface presents water of poor quality for irrigation (EC > 3 dS/m). The indicator kriging map shows a clear precision in the prediction of higher classes in groundwater salinity.

From the manager's perspectives, these results have important implications on the Lower-Cheliff plain's environmental and agriculture sustainability, while these water resources are used potentially for irrigation. Therefore, long-term use poses a potential risk for soil salinization and crops' productivity. First, the situation of the irrigated areas is assessed in the semiarid region of the Lower-Cheliff and the coming danger(s). Second, an accurate prediction of the groundwater salinity high classes is performed using the IK method. The accurately obtained spatial distribution with IK method can be a basis for developing a strategy to protect the cropping systems such as: drainage network, leaching dose, and crop tolerance to water salinity, against soil salinization.

The presented methodology based to IK interpolation is robust and could be applied to the risk analysis studies, where the spatial probability will be necessary for the evaluation of the potential effect on the environment, and then, the accuracy of the high value

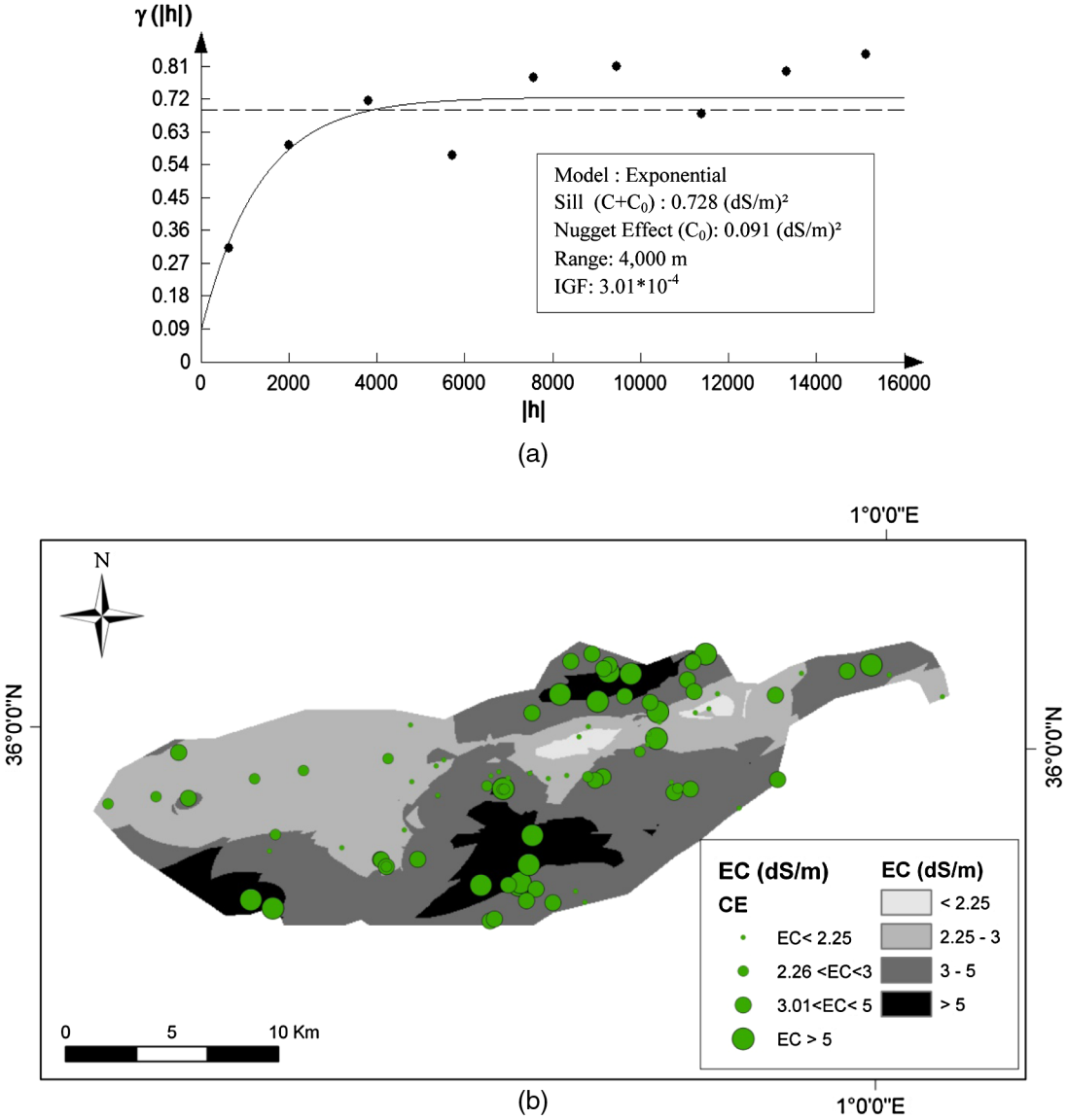

Fig. 7. (a) Variogram of the mathematical expectation; (b) prediction map of groundwater EC using IK

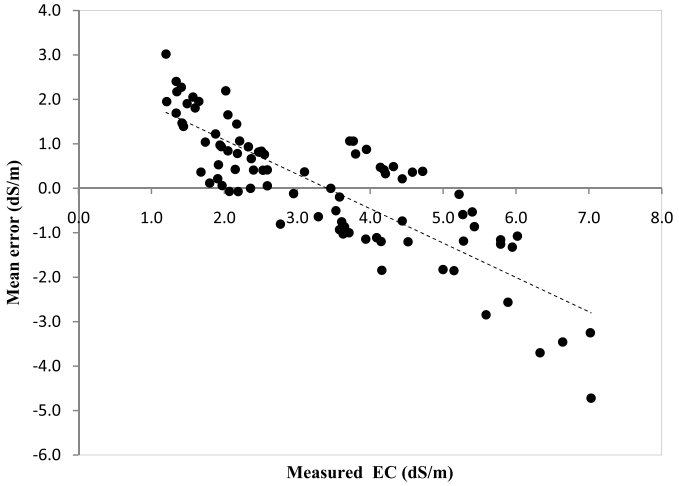

Fig. 8. Scatter plot of groundwater measured EC and the estimated residues using ordinary kriging

Table 5. Comparison of Surface Areas for EC Classes Estimated Using OK and Those from IK Prediction

	OK		IK	
Classes	Area (hm^2)	(%)	Area (hm^2)	(%)
EC < 2.25	1,768.25	5.81	471	1.55
2.25 < EC < 3	10,508.5	34.55	11,573	38.05
3 < EC < 5	15,927.25	52.37	14,448.5	47.51
EC > 5	2,208.5	7.26	3,920	12.89
Total	30,412.5	100	30,412.5	100

Table 6. Cross Validation for Both Ordinary and Indicator Kriging

Kriging method	ME	RMSE
OK	−0.0120	0.9210
IK	0.0092	0.0104

generally underestimating by the most spatial interpolated method used (OK).

Conclusion

The application of a robust interpolation method is important for the spatial analysis of groundwater salinity that is potentially used in irrigation. In this paper, the authors used an efficient approach for the prediction of groundwater salinity in the Lower-Chleff plain (Algeria) based on the IK methodology. This geostatistical method provides accuracy in the spatial distribution of groundwater salinity by estimating the probability of exceeding a threshold value. The combination of the CCDFs provides a good prediction of the EC high values and gave an accurate map for the high classes.

The variographic analysis shows that the indicator classes present a good spatial structuring. The spatial pattern of the EC groundwater in the plain of Lower-Cheliff revealed an advanced state of salinity risk using groundwater irrigation. Thus, using the OK estimated map shows 2% of the total surface in the region has salinity below 2.25 dS/m, whereas nearly 60% of this area has an EC higher than 3 dS/m. The use of IK has improved the mapping of groundwater salinity risk in the Lower-Cheliff with a better assessment of the areas through an optimization of the extreme values prediction (the problem of underestimation), and better precision by reducing the uncertainty. IK can be applied to generate estimation maps for irrigated zones with expected potential crops yield in the study area.

References

Adhikary, P. P., Dash, C. J., Bej, R., and Chandrasekharan, H. (2011). "Indicator and probability kriging methods for delineating Cu, Fe, and Mn contamination in groundwater of Najafgarh Block, Delhi, India." *Environ. Monit. Assess.*, 176(1–4), 663–676.

Akin, H., and Siemes, H. (1988). *Practical geostatistics: A primer for the mining and geosciences*, Springer, Berlin (in Deutsch).

Amichi, H., et al. (2012). "How does unequal access to groundwater contribute to marginalization of small farmers? The case of public lands in Algeria." *Irrig. Drain.*, 61(1), 34–44.

Antunes, I., and Albuquerque, M. (2013). "Using indicator kriging for the evaluation of arsenic potential contamination in an abandoned mining area (Portugal)." *Sci. Total Environ.*, 442, 445–552.

Arslan, H. (2012). "Spatial and temporal mapping of groundwater salinity using ordinary kriging and indicator kriging: The case of Bafra plain, Turkey." *Agric. Water Manage.*, 113, 57–63.

Assaf, H., and Saadeh, M. (2009). "Geostatistical assessment of groundwater nitrate contamination with reflection on DRASTIC vulnerability assessment: The case of the Upper Litani Basin, Lebanon." *Water Resour. Manage.*, 23(4), 775–796.

Ayers, R. S., and Wescot, D. W. (1988). *Water quality for agriculture*, Food and Agricultural Organization of the United Nations, Rome.

Bierkens, M. E. P., and Burrough, P. A. (1993). "The indicator approach to categorical data. I. Theory." *J. Soil Sci.*, 44(2), 361–368.

Bouarfa, S., et al. (2009). "Salinity patterns in irrigation systems, a threat to be demystified, a constraint to be managed: Field evidence from Algeria and Tunisia." *Irrig. Drain.*, 58(S3), S273–S284.

Bradaï, A., Douaoui, A., and Hartani, T. (2012). "Some problems of irrigation water management in Lower-Cheliff plain (Algeria)." *J. Environ. Sci. Eng. A*, A1(3A), 271–278.

Cambardella, C. A., et al. (1994). "Fields-scale variability of soil proprieties in central Iowa soils." *Soil Sci. Soc. Am. J.*, 58(5), 1501–1511.

Chica-Olmo, M., Luque-Espinar, J. A., Rodriguez-Galiano, V., Pardo-Iguzquiza, E., and Chica-Rivas, L. (2014). "Categorical indicator kriging for assessing the risk of groundwater nitrate pollution: The case of Vega de Granada aquifer (SE Spain)." *Sci. Total Environ.*, 470–471, 229–239.

Cressie, N. A. C. (1991). *Statistics for spatial data*, Wiley, New York.

Dash, J. P., Sarangi, A., and Singh, D. K. (2010). "Spatial variability of groundwater depth and quality parameters in the National Capital Territory of Delhi." *Environ. Manage.*, 45(3), 640–650.

Davis, B. M. (1984). "Indicator kriging as applied to an alluvial gold deposit." *Geostatistics for natural resources characterisation. Part I*, G. Verly, et al., eds., D. Reidel, 33, Springer, Berlin, 7–348.

Delhomme, J. P. (1978). "Kriging in the hydrosciences." *Adv. Water Resour.*, 1(5), 251–266.

Demir, Y., Ersahin, S., Güler, M., Cemek, B., Günal, H., and Arslan, H. (2008). "Spatial variability of depth and salinity of groundwater under irrigated ustifluvents in the Middle Black Sea region of Turkey." *Environ. Monit. Assess.*, 158(1), 279–294..

Deutsch, C. V., and Journel, A. G. (1998). *GSLIB. Geostatistical software library and user's guide*, Oxford University Press, New York.

Douaoui, A. E. K., Hervé, N., and Walter, C. (2006). "Detecting salinity hazards within a semiarid context by means of combining soil and remote sensing data." *Geoderma*, 134(1–2), 217–230.

Douaoui, A. E. K., and Lepinard, P. (2010). "Remote sensing and soil salinity: Mapping of soil salinity in the Algerian plain (Lower-Cheliff)." *Geomatics Expert*, 76, 36–41 (in French).

Douaoui, A. E. K., Walter, C., Gaouar, A., and Hammoudi, S. (2001). "Assessment of the topsoil structural degradation of the Lower-Cheliff

Valley (Algeria)." *4th Conf. of the Working Group on Pedometrics (WG-PM)*, Ghent, Belgium, 19–21.
Eldeiry, A. A., and Garcia, L. A. (2011). "Using indicator kriging technique for soil salinity and yield management." *J. Irrig. Drain. Eng.*, 10.1061/(ASCE)IR.1943-4774.0000280, 82–93.
Goovaerts, P., AvRuskin, G., Meliker, J., Slotnick, M., Jacquez, G., and Nriagu, J. (2005). "Geostatistical modeling of the spatial variability of arsenic in groundwater of southeast Michigan." *Water Resour. Res.*, 41(7), 1–19.
Goovaerts, P., and Journel, A. G. (1995). "Integrating soil map information in modelling the spatial variation of continuous soil properties." *Eur. J. Soil Sci.*, 46(3), 397–414.
Hartani, T., Bradaï, A., and Douaoui, A. E. K. (2012). "Exploring salinity perception in lower-Cheliff plain (Algeria)." *J. Agric. Sci. Technol.*, 2(11a), 1253–1259.
Hooshmand, A., Delghandi, M., Izadi, A., and Aali, K. A. (2011). "Application of kriging and cokriging in spatial prediction of groundwater quality parameters." *Afr. J. Agric. Res.*, 6(14), 3402–3408.
Journel, A. G. (1983). "Nonparametric estimation of spatial distributions." *J. Int. Assoc. Math. Geol.*, 15(3), 45–68.
Journel, A. G. (1986). "Geostatistics: Models and tools for the earth sciences." *Math. Geol.*, 18(1), 119–140.
Kasmaee, S., Gholamnejad, J., Yarahmadi, A., and Mojtahedzadeh, H. (2010). "Reserve estimation of the high phosphorous stockpile at the Choghart iron mine of Iran using geostatistical modeling." *Min. Sci. Technol.*, 20(6), 855–860.
Kuisi, M. A., Al-Qinna, M., Margani, A., and Aljazzar, T. (2009). "Spatial assessment of salinity and nitrate pollution in Amman-Zarqa basin: A case study." *J. Environ. Earth Sci.*, 59(1), 117–129.
Kumar, V. (2007). "Optimal contour mapping of groundwater levels using universal kriging—A case study." *Hydrol. Sci. J.*, 52(5), 1038–1050.
Lloyd, C. D., and Atkinson, P. M. (2001). "Assessing uncertainty in estimates with ordinary and indicator kriging." *Comput. Geosci.*, 27(8), 929–937.
Mendes, M. P., and Ribeiro, L. (2010). "Nitrate probability mapping in the northern aquifer alluvial system of the river Tagus (Portugal) using disjunctive kriging." *Sci. Total Environ.*, 408(5), 1021–1034.
Pannatier, Y. (1996). *VARIOWIN: Software for spatial data analysis in 2D*, Springer, New York.
Ramsis, B. S., Claus, J. O., and Robert, W. F. (1999). "Contributions of groundwater conditions to soil and water salinization." *Hydrogeol. J.*, 7(1), 46–64.
Richards, L. A. (1954). "Diagnosis and improvement of saline and alkali soils." USDA, Washington, DC.
Solow, A. R. (1993). "On the efficiency of the indicator approach in geostatistics." *Math. Geol.*, 25(1), 53–57.
Theodossiou, N., and Latinopoulos, P. (2007). "Evaluation and optimization of groundwater observation networks using the kriging methodology." *Environ. Modell. Software*, 21(7), 991–1000.
Triantafilis, J., Odeh, I O. A., Warr, B., and Ahmed, M. F. (2004). "Mapping of salinity risk in the lower Namoi valley using non-linear kriging methods." *Agric. Water Manage.*, 69(3), 203–231.
Verfaillie, E., Van Lancker, V., and Van Meirvenne, M. (2006). "Multivariate geostatistics for the predictive modelling of the surficial sand distribution in shelf seas." *Cont. Shelf Res.*, 26(19), 2454–2468.
Walter, C. (1993). "Comparison of soil properties using indicator kriging and soil map data." *Sci. du sol*, 31(4), 215–231.
Webster, R., and Oliver, M. A. (2001). *Geostatistics for environmental scientist*, Wiley, Chichester, England.
Yahiaoui, I., Douaoui, A. E. K., Zhang, Q., and Ziane, A. (2015). "Soil salinity prediction in the Lower Cheliff plain (Algeria) based on remote sensing and topographic feature analysis." *J. Arid Land*, 7(6), 795–805.
Yimit, H., Eziz, M., Mamat, M., and Tohti, G. (2011). "Variations in groundwater levels and salinity in the Ili River irrigation area, Xinjiang, northwest China: A geostatistical approach." *Int. J. Sustainable Dev. World Ecol.*, 18(1), 55–64.